Available online at www.sciencedirect.com
SCIENCE DIRECT®
International Journal of Solids and Structures 42 (2005) 1777–1795
INTERNATIONAL JOURNAL OF SOLIDS and STRUCTURES
www.elsevier.com/locate/ijsolstr

Effects of cell shape and cell wall thickness variations on the elastic properties of two-dimensional cellular solids

K. Li [a], X.-L. Gao [b,*], G. Subhash [a]

[a] *Department of Mechanical Engineering—Engineering Mechanics, Michigan Technological University, 1400 Townsend Drive, Houghton, MI 49931-1295, USA*
[b] *Department of Mechanical Engineering, Texas A&M University, 3123 TAMU, College Station, TX 77843-3123, USA*

Received 2 December 2003; received in revised form 9 August 2004
Available online 21 September 2004

Abstract

The Voronoi tessellation technique and the finite element method are utilized to investigate the microstructure-property relations of two-dimensional cellular solids having irregular cell shapes and non-uniform cell wall thickness. Twenty finite element models are constructed for each type of honeycomb samples (specimens) to obtain the mean values and standard deviations of the effective elastic properties. Spatially periodic boundary conditions are applied to each specimen containing 360 complete cells. The simulation results indicate that the elastic moduli increase as cell shapes become more irregular, but decrease as cell wall thickness gets less uniform. The Poisson's ratios are insignificantly affected by the presence of these two types of imperfections. The effect of the interaction between the co-existing cell shape and cell wall thickness imperfections on the elastic moduli is found to be weak. Bending remains as the dominant deformation mechanism in a loaded honeycomb having irregular cell shapes and/or non-uniform cell wall thickness. In addition, it is revealed that such imperfect honeycombs can be regarded as isotropic.

Keywords: Cellular solids; Irregular cell shapes; Non-uniform cell wall thickness; Voronoi tessellation; Finite element method

1. Introduction

Cellular solids (foams) are prevalent in nature and ubiquitous in engineering applications. Physical behaviors of such materials depend on the cell topology, the relative density and the properties of the cell wall material. A successful model that links the observed foam properties to the complex microstructures of

* Corresponding author. Tel.: +1 979 845 4835; fax: +1 979 845 3081.
E-mail address: xlgao@tamu.edu (X.-L. Gao).

0020-7683/$ - see front matter © 2004 Elsevier Ltd. All rights reserved.
doi:10.1016/j.ijsolstr.2004.08.005

foams can help us to understand how the microstructures affect the mechanical properties and enable us to optimize the microstructural parameters for a given application.

Many models, analytical or experimental, have been developed, based on idealized unit cells, to predict mechanical properties of cellular solids. An idealized unit cell (also called repeating unit) can capture the essential microstructural features of a typical cell extracted from a real cellular material. The repeating unit is usually a hexagonal cell when modeling two-dimensional (2-D), honeycomb-like foams. For three-dimensional (3-D) cellular materials, cubic, tetrahedral, dodecahedral and tetrakaidecahedral cells have been used as repeating units. With the simplified geometry of a unit cell, closed-form structure-property relations can be derived (e.g., Silva et al., 1995; Gibson and Ashby, 1997; Li et al., 2003a).

Although unit cell-based models can provide important results, they are significantly limited by their inability to account for microstructural imperfections inherent in most real cellular materials, whose cell structures are typically non-periodic, non-uniform and disordered. Thus, more complex, statistical models are necessitated to obtain improved predictions. To this end, suitable numerical methods are often required because of the stochastic nature of the problem.

Efforts have been made to investigate the effects of imperfections, such as irregular cell shapes, non-uniform cell wall thickness, wavy cell walls, and missing or fractured cell walls, on mechanical properties of cellular materials; most of these studies are based on the finite element method (FEM). For example, Silva et al. (1995) generated non-periodic arrays of 2-D Voronoi cells with uniform cell wall thickness, and found that the irregularity of cell shapes does not introduce significant variance in the elastic properties of low-density honeycombs. The effect of material distribution in the cell edges of hexagonal honeycombs on the stiffness and strength of metallic foams was investigated by Simone and Gibson (1998a). Their finite element results indicated that the modulus and peak stress of a metallic honeycomb initially increase and then decrease as the material shifts away from the cell edges into Plateau borders near the vertices. Simone and Gibson (1998b) also studied the influence of edge/face curvature and corrugations on the properties of hexagonal honeycombs, where they showed that wavy distortions substantially reduce the effective modulus and peak stress of a honeycomb. The study of Silva and Gibson (1997) revealed that random cell wall removals sharply lower the effective mechanical properties of both perfect and imperfect honeycombs. Among the random imperfections considered in Chen et al. (1999), i.e., cell size variations, fractured cell walls, cell wall misalignments and missing cells, fractured cell edges were found to cause the biggest reduction in yield strength of 2-D foams. More recently, Fazekas et al. (2002) studied the effects of cell shape variations on the Young's modulus and yield strength of 2-D cellular solids and found that the cell geometry has a large influence on the mechanical properties of the cellular solids. However, in each of the studies mentioned above only one type of imperfections was included at a time. In general, two or more types of imperfections are simultaneously involved in the microstructure of a cellular material. Therefore, models incorporating two or more types of imperfections are still in need.

The objective of this paper is to address the combined effects of two co-existing imperfections—irregular cell shapes and non-uniform cell wall thickness—on the elastic properties of 2-D foams. The rest of this paper is organized as follows. In Section 2, honeycombs with different degrees of cell shape irregularity (amplitude a) and cell wall thickness non-uniformity (amplitude b) are first constructed using the Voronoi tessellation technique. Twenty finite element (FE) models are then developed for each type of honeycombs having the same pair of a and b by using the constructed Voronoi diagrams to calculate the effective Young's moduli, Poisson's ratios and shear modulus of the honeycombs. Each of these diagrams (specimens) contains 360 complete cells. In Section 3, a mesh sensitivity study is first performed to determine the appropriate number of cells to be included in each specimen, and the choice of 20 specimens to be used in the statistical analysis is then justified. This is followed by an investigation into the elastic behavior (isotropic or anisotropic) of the honeycombs based on the Voronoi diagrams and the FE models. Finally, a parametric study for sample cases involving different values of the cell shape irregularity amplitude, the cell wall thickness non-uniformity amplitude, and the relative foam density is conducted, with the simulation results presented and discussed. A summary is given in the fourth and last section.

2. Analysis

The Voronoi tessellation technique is often used to capture random features of foam microstructures. When a set of seeds, placed in space simultaneously in a random fashion, grow in all directions with a uniform speed, a 2-D or 3-D Voronoi diagram is formed, depending on the space dimension. The Voronoi tessellation structure is fully determined by the initial locations of the seeds (e.g., Glaessgen et al., 2003). Using regularly positioned seeds produces regular Voronoi diagrams. The current analysis starts with a reference model, which is a hexagonal honeycomb structure with perfectly ordered, regular cell shapes and uniform cell wall thickness. This reference model can be constructed from a set of regularly packed seeds using the Voronoi tessellation technique, as shown in Fig. 1. Perturbations are then introduced to the reference model to generate Voronoi diagrams with irregular cell shapes and non-uniform cell wall thickness. The non-uniformity here and in the sequel means that the thickness of one cell wall may differ from that of any other cell wall, although each cell wall is regarded as having the same thickness.

2.1. Spatially periodic honeycombs with cell shape and cell wall thickness variations

There are two methods to construct 2-D random foam models using the Voronoi tessellation technique. The first method starts with building a Voronoi tessellation that is larger than the foam specimen of interest from a set of randomly placed seeds. Then, a bounding rectangle with dimensions same as those of the specified foam specimen is imposed to trim off the extraneous layer of the tessellation (e.g., Van der Burg et al., 1997). This layer contains Voronoi cells that do not resemble (even irregular) cells of a honeycomb. It should be noted that the model so obtained is not periodic and many cells must be included in the specimen to minimize the edge effect. In addition, only displacement boundary conditions can be applied in this case. The second method is to use a set of seeds of periodic symmetry (e.g., Nygards and Gudmundson, 2002). First, a preset number of seeds are generated within a rectangle. Then, the position of each seed within the rectangle is copied to eight identical rectangles adjacent to or sitting at the corners of the original rectangle. Finally, the Voronoi tessellation technique is applied to all of the seeds within the nine rectangles. Part of the resulting Voronoi tessellation that is inscribed by the center (original) rectangle can be taken out as a periodic specimen. In this study, the second method is adopted to generate seeds of periodic symmetry, and the needed Voronoi diagrams are then constructed using the program Qhull developed at the Geometry Center, the University of Minnesota—Twin Cities (now available at http://www.geom.uiuc.edu/software/qhull/).

The irregularity of cell shapes is determined by the irregular distribution of the seeds. The locations of the seeds used to construct Voronoi diagrams with irregular cell shapes are perturbed from a regular lattice

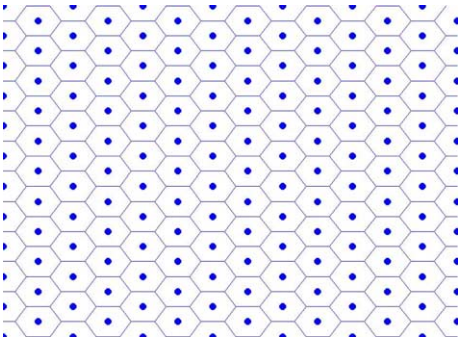

Fig. 1. Voronoi diagram based on regularly packed seeds.

of seeds. Fig. 2 shows the coordinate perturbations of a regularly packed seed. The perturbed coordinates of seed i, x_1^i and x_2^i, may be represented by

$$\begin{aligned} x_1^i &= \bar{x}_1^i + a(d_0 \cos\theta_i)\varphi_i, \\ x_2^i &= \bar{x}_2^i + a(d_0 \sin\theta_i)\varphi_i, \end{aligned} \tag{1}$$

where $\bar{x}_1^i$, $\bar{x}_2^i$ are the two coordinates of the same seed in the regular lattice, d_0 is the distance between two regularly packed (unperturbed) seeds, θ_i ($\in[0,2\pi]$) is a stochastic angle (with a uniform distribution) between the x_1-axis and the line connecting the unperturbed and perturbed seeds, φ_i ($\in[-1,1]$) is a random variable with a uniform distribution, and a ($\in[0,1]$) is the amplitude used to quantify the degrees of cell shape irregularity. The smaller a is, the more regular the Voronoi diagram is. Regular hexagonal honeycombs are obtained when $a=0$, and completely irregular honeycombs are defined when $a=1.0$. Fig. 3 shows honeycomb samples with different degrees of cell shape irregularity. Each sample includes 360 complete cells. It should be pointed out that the expressions given in Eq. (1) for locating the perturbed seed involve the stochastic angle θ_i and differ from the ones used in the earlier studies reviewed in Section 1.

For given relative density and amplitude of cell shape irregularity, the predicted properties of a honeycomb having uniform cell wall thickness depend on the two sets of stochastic variables θ_i and φ_i ($i\in\{1,\ldots,M\}$; $M=$ the total number of seeds) (see Eq. (1)), which are produced using two different generators of uniformly distributed random numbers. To obtain the expectation values of the foam properties, a significant number of simulations with various sets of θ_i and φ_i are therefore needed. In this study, 20 samples are analyzed for each value of a in order to compare with the results presented in Silva et al. (1995). The choice of 20 specimens (samples) will be discussed further in Section 3.

After the cell shapes are determined, statistical thickness variations can be introduced to the uniform cell wall thickness t_0:

$$t_0 = \frac{RL_1L_2}{\sum_{j=1}^{N} l_j}, \tag{2}$$

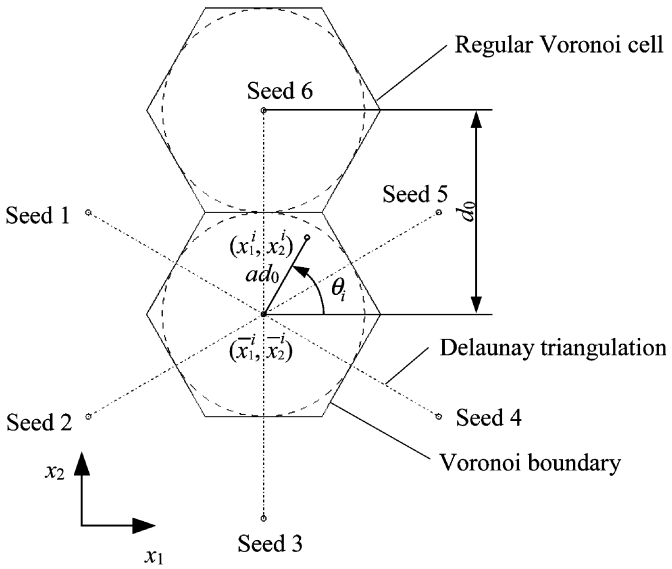

Fig. 2. Coordinate perturbations of the ith seed ($\bar{x}_1^i$, $\bar{x}_2^i$).

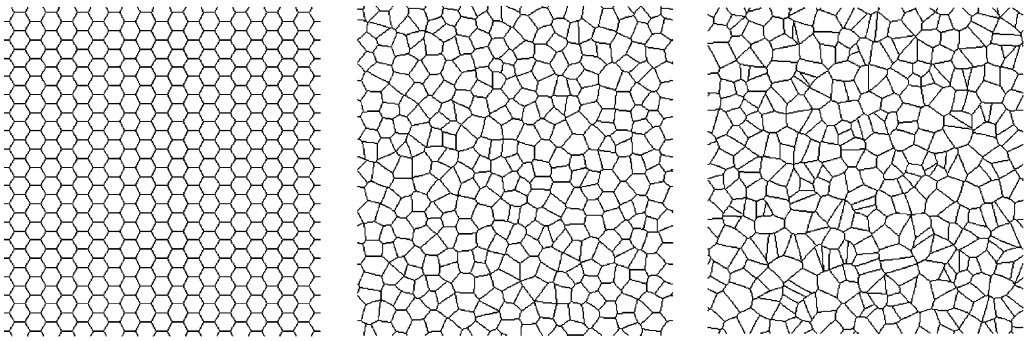

Fig. 3. Honeycomb samples with varying a: (a) $a = 0$, (b) $a = 0.5$, (c) $a = 1.0$.

where R is the relative foam density, L_1 and L_2 are, respectively, the width and height of the foam sample (specimen), l_j is the length of cell wall j, and N is the total number of cell walls. To this end, each cell wall is assigned a random thickness given by (e.g., Grenestedt and Bassinet, 2000)

$$t_j = ct_0(1 + b\psi_j), \tag{3}$$

where b ($\in [0,1]$) is the amplitude used to quantify the non-uniformity of cell wall thickness, ψ_j ($\in [-1,1]$) is a random variable with a uniform distribution, and c, called the normalizing factor, is defined by

$$c = \frac{\sum_{j=1}^{N} l_j}{\sum_{j=1}^{N}(1 + b\psi_j)l_j} \tag{4}$$

to ensure that the relative density (R) remains unchanged with the variation of the cell wall thickness. Given R, a, b, θ_i and φ_i ($i \in \{1,\ldots,M\}$), the predicted foam properties depend on the set of random variables ψ_j ($j \in \{1,2,\ldots,N\}$), which are generated independently of θ_i and φ_i ($i \in \{1,2,\ldots,M\}$). Statistically, it is required to run sufficient simulations with different sets of ψ_j to obtain the expectation values of the foam properties. In this study, 20 foam samples (specimens), with a remaining fixed for each sample, will be analyzed for each given value of b. The reason for choosing 20 specimens will be provided in Section 3.

2.2. Finite element analyses

A finite element study is performed to obtain the elastic properties of honeycombs with cell shape and cell wall thickness variations using the commercial software package ABAQUS 6.3 (Hibbitt et al., 2002). Here, graphitic carbon foams are considered, whose modeling partially motivated this study. The Young's modulus E_s and Poisson's ratio v_s of the solid carbon material are, respectively, taken to be 15.61 GPa and 0.33 (Li et al., 2003a,b). Each cell wall is modeled with a three-node beam element (element type B22 in ABAQUS), which involves bending, stretching and shearing deformation mechanisms. An earlier study by Silva et al. (1995) showed that using such a beam element to model each cell wall was sufficient for convergence. It is noted that exceptionally short cell walls exist in honeycomb specimens having highly irregular cell shapes. Typical beam elements cannot well represent these short cell walls (e.g., Silva et al., 1995). However, since short cell walls only account for a small fraction (a few percent) of the total number of cell walls, the effect incurred from using inappropriate element types is negligible (Van der Burg et al., 1997; Chen et al., 1999). Deletion of short cell walls in the finite element model may even reduce the degrees of freedom of the model, thereby resulting in overestimated stiffness for the honeycomb (Silva et al., 1995).

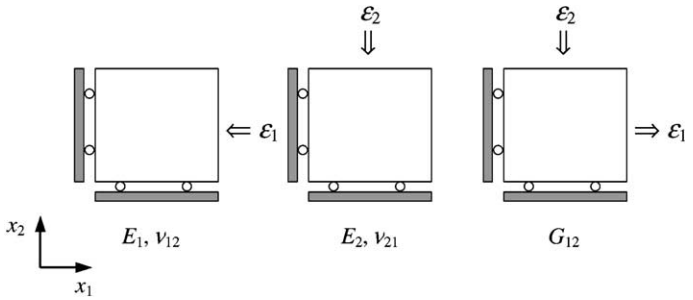

Fig. 4. Simulated tests for determining the effective properties.

Uniaxial compressive tests on honeycomb specimens along two orthogonal directions, x_1 and x_2, are considered in two separate analyses to obtain the effective Young's moduli and Poisson's ratios of the honeycomb relative to the two directions (see Fig. 4). In each analysis, a small compressive strain in the amount of -0.001 is applied in the loading direction to ensure elastic deformations needed. The effective Young's moduli E_1 and E_2 of the honeycomb are then obtained as

$$E_1 = \frac{-F_1}{h\varepsilon_1 L_2}, \tag{5}$$

$$E_2 = \frac{-F_2}{h\varepsilon_2 L_1}, \tag{6}$$

where h is the thickness of the honeycomb, ε_1 and ε_2, both being -0.001, are the applied compressive strains, and F_1 and F_2 are, respectively, the total reaction forces along x_1 and x_2 directions on the prescribed boundary. Also, the effective Poisson's ratios are obtained as

$$\nu_{12} = -\frac{u_2}{\varepsilon_1 L_2}, \tag{7}$$

$$\nu_{21} = -\frac{u_1}{\varepsilon_2 L_1}, \tag{8}$$

where u_1 and u_2 are the lateral displacements (extensions) perpendicular to the loading directions x_2 and x_1, respectively.

To determine the effective shear modulus, a biaxial loading test is simulated. A small tensile strain $\varepsilon_1 = 0.001$ in the x_1 direction and a small compressive strain $\varepsilon_2 = -0.001$ in the x_2 direction are applied simultaneously (see Fig. 4). Then, the effective shear modulus G_{12}, defined by $G_{12} = \tau_{12}/\gamma_{12}$, is determined as

$$G_{12} = \frac{F_1/L_2 - F_2/L_1}{2h(\varepsilon_1 - \varepsilon_2)}, \tag{9}$$

where F_1 and F_2 are obtained from the finite element analysis.

In modeling uniaxial or biaxial loading tests, displacement boundary conditions are usually used (e.g., Silva et al., 1995; Silva and Gibson, 1997; Van der Burg et al., 1997; Simone and Gibson, 1998a,b; Fazekas et al., 2002). For instance, displacement constraints may be imposed at the bottom nodes of the specimen in the x_2 direction and at the nodes on the left side of the specimen in the x_1 direction, if strains are applied on the top and/or right sides of the specimen, as shown in Fig. 4. However, since the specimen is cut out of an infinite structure that can be regarded as periodic, spatially periodic boundary conditions should be applied to ensure that the predicted properties of the specimen are representative of those of the honeycomb

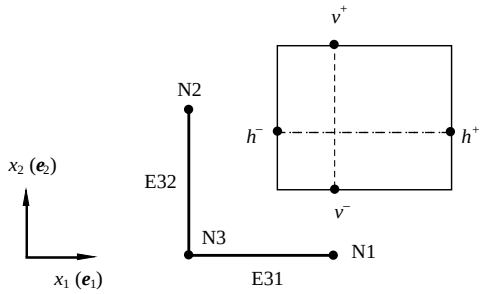

Fig. 5. Matched nodes for implementing spatially periodic boundary conditions.

(Laroussi et al., 2002). Displacement boundary conditions that only restrain normal displacements may underestimate foam properties (Chen et al., 1999). The specimen obtained by following the procedure described in Section 2.1 (for the second method) is periodic, i.e., each node on one side (e.g., v^-) has a matched node on the opposite side of the specimen (e.g., v^+), as shown in Fig. 5. For a uniaxially deformed specimen subjected to prescribed strain ε_i, the periodic boundary conditions may be represented by

$$u_i^{k^+} - u_i^{k^-} = \varepsilon_i (x_i^{k^+} - x_i^{k^-}), \quad i \in \{1,2\}; \quad \omega^{k^+} - \omega^{k^-} = 0, \tag{10}$$

where x_i^{k+} and x_i^{k-} are, respectively, the positions of the matched nodes k^+ and k^- on the specimen boundary lines with outward unit normal vectors $\boldsymbol{e}_i$ and $-\boldsymbol{e}_i$, u_i^{k+} and u_i^{k-} are, respectively, the normal displacement components of k^+ and k^-, and ω^{k+} and ω^{k-} are, respectively, the rotations of k^+ and k^-. The periodic boundary conditions described in Eq. (10) have also been used in Chen et al. (1999), Nygards and Gudmundson (2002) and Laroussi et al. (2002).

The periodic boundary conditions given in Eq. (10) can be implemented by using the option EQUATION in ABAQUS and by introducing three reference nodes N1, N2 and N3, which define two two-node AXIAL connector elements E31 and E32 (see Fig. 5). Elements E31 and E32 intersect at reference node N3 and are located along the $\boldsymbol{e}_1$ and $\boldsymbol{e}_2$ directions, respectively. Node N1 is allowed to move axially only along element E31, and node N2 only along element E32. The degrees of freedom of the matched nodes may be coupled with those of the reference nodes by

$$u_i^{k^+} - u_i^{k^-} - \frac{x_i^{k^+} - x_i^{k^-}}{X_i^{K^+} - X_i^{K^-}} (U_i^{K^+} - U_i^{K^-}) = 0, \quad \omega^{k^+} - \omega^{k^-} - (\Omega^{K^+} - \Omega^{K^-}) = 0, \tag{11}$$

where X_i, U_i ($i \in \{1,2\}$) and Ω are, respectively, the positions, displacements and rotations of the reference nodes, the superscript "K^+" denotes reference nodes N1 and N2, and the superscript "K^-" stands for reference node N3. For uniaxial compression along $-\boldsymbol{e}_2$, say, node N3 is fixed and a displacement corresponding to $\varepsilon_2 = -0.001$ is applied at node N2. The reaction force induced in element E32, called ETF1 in ABAQUS, can be substituted into Eq. (6) for F_2, and the axial displacement of element E31, called EU1 in ABAQUS, can be inserted into Eq. (8) for u_1. It has been found that the procedure described here, which utilizes the two end nodes of a connector element as the reference nodes, is easier to implement than that introduced earlier by Laroussi et al. (2002), where a pair of matched nodes located on two opposite boundary surfaces of a 3-D regular open-cell foam specimen were employed in each loading direction.

To investigate the effects of using different types of boundary conditions, a group of regular honeycomb specimens are modeled. The group consists of four specimens similar to the one shown in Fig. 3(a) but with varying number of cells. All of the four specimens have the same relative density $R = 0.01$. The elastic properties predicted using the displacement boundary conditions (DBCs) and periodic boundary conditions (PBCs), respectively, are listed in Table 1. According to Gibson and Ashby (1997), the effective Young's

Table 1
Comparison of different boundary conditions

	$n_1 \times n_2$[a]	E_1 (kPa)	v_{12}	E_2 (kPa)	v_{21}	E_1/E_2	v_{12}/v_{21}
DBCs	6×8	19.1895	0.8197	23.4048	0.9997	0.8199	0.8199
	9×12	20.6317	0.8813	23.4046	0.9997	0.8815	0.8816
	18×20	22.0328	0.9411	23.4046	0.9997	0.9414	0.9414
	21×24	22.2322	0.9496	23.4046	0.9997	0.9499	0.9499
PBCs	6×8	23.4041	0.9997	23.4041	0.9997	1	1
	9×12	23.4041	0.9997	23.4041	0.9997	1	1
	18×20	23.4042	0.9997	23.4042	0.9997	1	1
	21×24	23.4033	0.9997	23.4033	0.9997	1	1

[a] n_1 and n_2 are, respectively, the number of cells in the x_1- and x_2-directions.

moduli and Poisson's ratios of a regular honeycomb in its two orthogonal directions are equivalent, and their values are independent of the number of cells. As shown in Table 1, the properties obtained using the PBCs are indeed independent of the number of cells used, thereby agreeing with what was noted in Gibson and Ashby (1997). In contrast, the results predicted using the DBCs vary with the cell number and indicate that the isotropy of the honeycomb is enhanced as the number of cells increases. This comparison shows that the PBCs can better capture the mechanical behavior of honeycombs. Hence, they are employed in our finite element simulations discussed below.

3. Results and discussions

3.1. Mesh sensitivity

Before proceeding to model honeycombs having irregular cell shapes and non-uniform cell wall thickness, an important issue that needs to be resolved is to determine the appropriate number of cells (C) to be included in a specimen and the appropriate number of specimens (S) to be analyzed for each type of honeycombs. Based on a finite element analysis of random heterogeneous materials using representative volume elements (RVEs) of various sizes, Kanit et al. (2003) found that for a given precision the effective elastic properties of the materials can be obtained through using either a large RVE accompanied by a small number of specimens or a small RVE accompanied by a large number of specimens. This indicates that the number of specimens needs to be carefully chosen for accurate predictions. As mentioned earlier, in the current study the number of specimens is initially taken to be 20 (i.e., $S = 20$) for each type of honeycombs to be simulated, which is the same as that used in Silva et al. (1995). Nine families of specimens, each family containing a same number of cells C ($C \in \{48, 108, 144, 192, 240, 300, 360, 432, 504\}$), are then considered to determine the appropriate C. For each family, 20 specimens are modeled to obtain the mean values (m) and standard deviations (δ) of the effective properties. The shape irregularity amplitude (a) and the relative density (R) remain to be 0.5 and 0.01, respectively, for all of the nine families of specimens. The pertinent numerical results are listed in Table 2.

From Table 2, it is seen that as the number of cells (C) increases, the mean values of the two effective Young's moduli (E_1, E_2) and the effective shear modulus (G_{12}) all decrease initially and then stay, respectively, at around 26 kPa and 6.6 kPa with small variations, while those of the effective Poisson's ratios (v_{12} and v_{21}) are insignificantly affected. The standard deviations (δ) of all the five properties are generally decreasing with the increase of C. When $C = 360$, δ is small for all of the five properties. Further increase of C does not lower the values of δ. Therefore, $C = 360$ is chosen as the number of cells to be included in a specimen.

Table 2
Effects of the number of cells on elastic properties

C	E_1 (kPa)		v_{12}		E_2 (kpa)		v_{21}		G_{12} (kpa)	
	m	δ	m	δ (10^{-5})	m	δ	m	δ (10^{-5})	m	δ
48	31.57	5.589	0.9996	7.446	31.57	5.583	0.9996	7.520	7.894	1.398
108	29.00	3.447	0.9996	4.219	29.00	3.446	0.9996	5.878	7.276	0.829
144	28.92	2.313	0.9996	3.843	28.92	2.313	0.9996	5.196	7.231	0.579
192	27.35	2.337	0.9996	3.304	27.35	2.337	0.9996	3.596	6.839	0.584
240	26.54	1.915	0.9996	2.796	26.54	1.915	0.9996	2.796	6.636	0.479
300	26.60	1.464	0.9996	2.230	26.60	1.464	0.9996	2.552	6.650	0.366
360	26.55	1.181	0.9996	1.759	26.55	1.181	0.9996	1.538	6.638	0.295
432	25.63	1.134	0.9996	1.789	25.63	1.134	0.9996	1.731	6.410	0.284
504	26.34	1.443	0.9996	2.124	26.35	1.438	0.9996	2.173	6.587	0.361

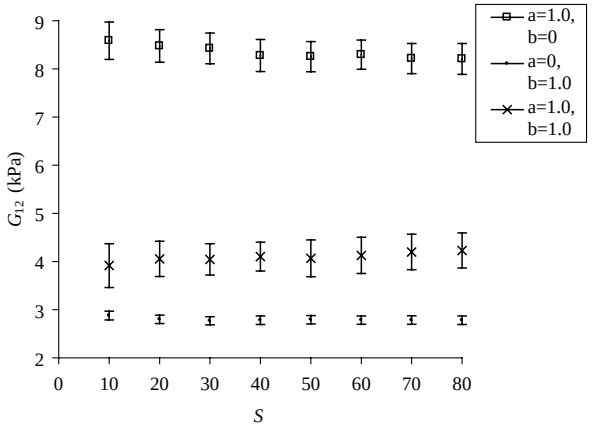

Fig. 6. The shear modulus varying with the number of specimens.

In order to evaluate whether the initially chosen number of specimens ($S = 20$) is an appropriate one, finite element analyses are conducted on three types of honeycombs: the completely irregular honeycombs with a uniform cell wall thickness ($a = 1.0, b = 0$), the regular honeycombs with completely non-uniform cell wall thickness ($a = 0, b = 1.0$), and the completely irregular honeycombs with completely non-uniform cell wall thickness ($a = 1.0, b = 1.0$). Each specimen contains 360 cells. The mean values (m) and standard deviations (δ) of the effective shear modulus G_{12} are obtained for the three types of honeycombs using various values of S ($S \in \{10, 20, 30, 40, 50, 60, 70, 80\}$), which are shown in Fig. 6. It is seen from Fig. 6 that the mean values of G_{12} change little with the variation of S. In addition, there is only a small change in the standard deviations of G_{12} as S increases from 10 to 20, and further increase of S does not lead to any significant change in the values of δ. Hence, the initial choice of $S = 20$ as the number of specimens is appropriate.

3.2. Isotropy of the effective properties

A total of 29 cases as listed in Table 3 are analyzed here. Controlling parameters include the degree of cell shape irregularity (amplitude a), the degree of cell wall thickness non-uniformity (amplitude b) and the

Table 3
Isotropy of elastic properties

R	a	b	E_1/E_2		v_{12}/v_{21}		G_{12}/G_{12}^T	
			m	δ	m	δ	m	δ
0.01	0	0	1	0	1	0	1	0
0.01	0.2	0	0.99999933	5.33443E−06	0.99999950	2.23669E−06	1	8.47180E−06
0.01	0.5	0	0.99999923	1.08169E−05	1.00000150	9.88449E−06	0.99999894	7.11786E−06
0.01	0.8	0	0.99999197	3.91625E−05	1.00000150	2.52012E−05	0.99999741	2.11883E−05
0.01	1.0	0	0.99997741	8.57673E−05	0.99997347	7.94084E−05	1.00000031	2.81441E−05
0.01	0	0.2	1	0	0.99999950	2.23673E−06	1.00000169	6.49030E−06
0.01	0	0.5	1.00000082	7.03450E−06	1.00000200	6.96030E−06	0.99554113	0.01995825
0.01	0	0.8	0.99999865	1.46421E−05	0.99999550	1.05030E−05	1.00000471	1.25045E−05
0.01	0	1.0	1.00099455	0.00248268	1.00099626	0.00249484	1.00066102	0.00195853
0.01	1.0	0.2	0.99998208	9.28584E−05	0.99997697	9.14235E−05	0.99999827	3.14686E−05
0.01	1.0	0.5	1.00001497	1.05325E−04	1.00001303	1.05629E−04	1.00000428	2.78819E−05
0.01	1.0	0.8	0.99929762	0.00331706	0.99929493	0.00331722	1.00021947	0.00090569
0.01	1.0	1.0	1.00072631	0.00190331	1.00072454	0.00190065	1.02207486	0.09696343
0.06	0	0	1	0	1	0	1	0
0.11	0	0	1	0	1	0	1	0
0.16	0	0	1	0	1	0	1	0
0.22	0	0	1	0	0.99998865	0	1	0
0.06	1.0	0	0.99978203	6.24103E−04	0.99977820	6.30239E−04	0.99994557	0.00014991
0.11	1.0	0	0.99923511	0.00187065	0.99933323	0.00183054	0.99970015	0.00048927
0.16	1.0	0	0.99870575	0.00321035	0.99874528	0.00321949	0.99965772	0.00079261
0.22	1.0	0	0.99800125	0.00481364	0.99798321	0.00478462	0.99947678	0.00128829
0.06	0	1.0	1.00134033	0.00944197	1.00153983	0.00944104	1.00088287	0.00339788
0.11	0	1.0	1.00496522	0.01237428	1.00496534	0.01237851	1.00165918	0.00320799
0.16	0	1.0	0.99780330	0.01836028	0.99785392	0.01840395	0.99984946	0.00460569
0.22	0	1.0	1.00480270	0.02282950	1.00479213	0.02286372	1.00171102	0.00613748
0.06	1.0	1.0	1.00164240	0.01729311	1.00163683	0.01728644	1.00148782	0.00489667
0.11	1.0	1.0	0.99703282	0.02023367	0.99705114	0.02022494	0.99983544	0.00526793
0.16	1.0	1.0	1.00197181	0.02909143	1.00195956	0.02907130	1.00129983	0.00794406
0.22	1.0	1.0	0.99695179	0.03263665	0.99695285	0.03266670	0.99976374	0.00954108

relative density (R). Except for the cases with $a = 0$ and $b = 0$ (totaling 5), the mean values and standard deviations of the elastic properties for each case listed in Table 3 are obtained from the results of the finite element analyses performed on 20 specimens. For the former (i.e., perfect honeycombs with different values of R), only one specimen is needed in each case. The mean ratios of E_1/E_2 and v_{12}/v_{21} and their standard deviations are given in Table 3. To examine whether the shear relation $G = E/[2(1 + v)]$ is satisfied, which is required for material isotropy, the mean ratios of G_{12}/G_{12}^T and their standard deviations are also listed in Table 3, where the values of G_{12}^T are obtained using $G_{12}^T = E_1/[2(1 + v_{12})]$. An inspection of Table 3 indicates that the standard deviations increase with a, b and R, while the mean values of E_1/E_2, v_{12}/v_{21} and G_{12}/G_{12}^T are very close to unity for all cases. Therefore, it can be concluded that the elastic response of the honeycombs studied is isotropic regardless of changes in cell shape irregularity, cell wall thickness non-uniformity and relative density.

3.3. Effects of cell shape irregularity

For regularly packed hexagonal cell honeycombs the general formulas provided in Silva et al. (1995) (see their Eqs. (4a–4d)), based on the unit cell method and incorporating cell wall bending, stretching and shearing deformation mechanisms, can be reduced to

$$E^* = \frac{1.5E_s R^3}{1 + (4.05 + 1.125v_s)R^2}, \tag{12}$$

$$v^* = \frac{1 + (1.05 + 1.125v_s)R^2}{1 + (4.05 + 1.125v_s)R^2}, \tag{13}$$

$$G^* = \frac{0.375E_s R^3}{1 + (2.2875 + 1.3125v_s)R^2}, \tag{14}$$

where E^*, v^* and G^* are, respectively, the effective Young's modulus, Poisson's ratio and shear modulus. An examination of Eqs. (12)–(14) shows that the shear relation, $G^* = E^*/[2(1 + v^*)]$, is not exactly satisfied by these three expressions. Nevertheless, the substitution of Eqs. (12) and (13) into the shear relation $G^* = E^*/[2(1 + v^*)]$ yields

$$G^* = \frac{0.375E_s R^3}{1 + (2.55 + 1.125v_s)R^2}, \tag{15}$$

which is very similar to the expression given in Eq. (14). In particular, this shear relation based expression, Eq. (15), leads to numerical values that are extremely close to those predicted by using Eq. (14) for the relative density range (i.e., $R = 0$–0.22) considered in the current study. For instance, when $R = 0.22$ (the largest value in the range), Eq. (15) gives a value of 0.05461 GPa, which is close to 0.05508 GPa, the value obtained using Eq. (14). The differences become even smaller for smaller values of R. Hence, the closed-form expressions given in Eqs. (12)–(14) are employed here to model isotropic behavior of perfect honeycombs.

When $R = 0.01$, Eqs. (12)–(14) give $E^* = 23.4045$ kPa, $v^* = 0.9997$ and $G^* = 5.85216$ kPa for a perfect honeycomb, while the results predicted by the finite element analysis for the specimen shown in Fig. 3(a) (i.e., the case with $C = 360$) are $E_1 = E_2 = 23.4042$ kPa, $v_{12} = v_{21} = 0.9997$ and $G_{12} = 5.85193$ kPa. It is clear that the elastic properties predicted by the unit cell method of Silva et al. (1995) and the current finite element model are almost the same for a perfect honeycomb.

The effects of irregular cell shapes on elastic properties are analyzed for honeycombs having a fixed relative density $R = 0.01$ and some uniform cell wall thickness (i.e., $b = 0$). For each value of a, 20 independent lists of random variables θ_i and φ_i ($i \in \{1, \ldots, M\}$) are used to generate 20 honeycomb samples, each of which has a unique arrangement of cell walls. Finite element analyses are then conducted on the 20 samples, and the mean values and standard deviations of the effective properties, i.e., the Young's moduli, Poisson's ratios and shear modulus, are obtained.

Figs. 7–9 graphically show the predicted elastic properties at different values of a. An examination of these three figures indicates that all the properties become more scattered as cell shapes become more irregular. When $a = 1.0$, the relative deviations (i.e., standard deviation/mean value) are 7.99003% for E_1,

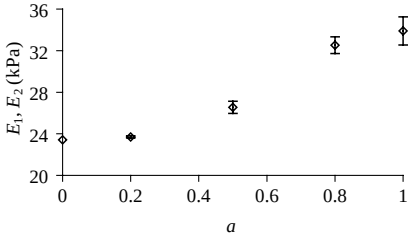

Fig. 7. Effects of cell shape irregularity on the Young's moduli (with $R = 0.01$).

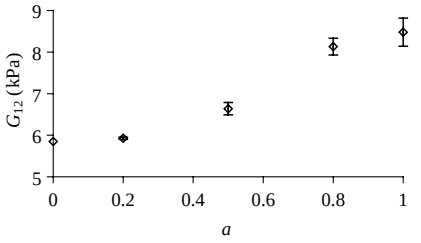

Fig. 8. Effects of cell shape irregularity on the shear modulus (with $R = 0.01$).

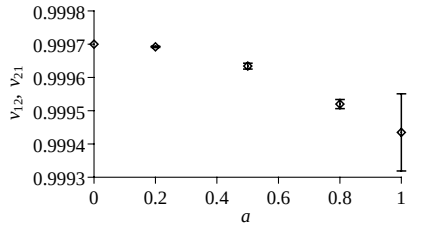

Fig. 9. Effects of cell shape irregularity on the Poisson's ratios (with $R = 0.01$).

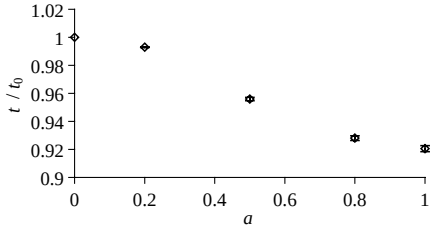

Fig. 10. Effects of cell shape irregularity on the cell wall thickness (with $R = 0.01$).

0.0307072% for v_{12}, 7.98939% for E_2, 0.0232045% for v_{21} and 7.99106% for G_{12}. From Figs. 7 and 8 it is observed that, on average, the elastic moduli increase considerably with a. The mean values of E_1, E_2 and G_{12} are approximately 45% larger when $a = 1.0$ than their corresponding values when $a = 0$. The regular honeycomb (with $a = 0$) is the weakest in terms of the elastic moduli. Poisson's ratios, however, are insignificantly affected by the cell shape irregularity, as shown in Fig. 9. Fig. 10 indicates the reduction of cell wall thickness with the increase of a, which undermines the moduli. The strong dependence of the moduli on a is attributed to the changes in the microstructure as cells become less regular. In addition to hexagons, other types of polyhedrons, such as pentagons, quadrangles and triangles, appear in the microstructure, as shown in Figs. 3(b) and (c). The stiffness of each of these fewer-sided polyhedrons is higher than that of a hexagon, and the stiffening effect associated with the appearance of fewer-sided polyhedrons substantially outweighs the loss in stiffness due to the small decrease in the wall thickness, thereby leading to a significant increase of the elastic moduli.

The study of Silva et al. (1995) did not deal with honeycombs with varying degrees of cell shape irregularity. The models they used are similar to the ones generated here with $a = 0.5$ (see Fig. 3(b)). Also, based on 20 samples, they predicted the elastic properties of isotropic, non-periodic honeycombs having a

constant relative density ($R = 0.15$). The relative deviations they found are approximately 6%, 4% and 9% for the Young's moduli, Poisson's ratios and shear modulus, respectively. For the random honeycombs, their findings indicate that the mean Young's moduli are 6% higher, the mean Poisson's ratios 1% lower, and the mean shear modulus 11% higher than their corresponding values for the perfect honeycomb. To compare with their results, we analyze one perfect honeycomb specimen with $a = 0$, $b = 0$ and 20 irregular specimens having $a = 0.5$, $b = 0$ and $R = 0.15$. Smaller relative deviations are obtained for the irregular honeycomb specimens, which are, respectively, 3.5% for the Young's moduli, 3.7% for the shear modulus, and 0.35% for the Poisson's ratios. The mean values of the Young's moduli, Poisson's ratios and shear modulus predicted in the current study are, respectively, 6.4% higher, 1.1% lower and 7.7% higher for the irregular specimens than their corresponding values for the perfect honeycomb. The differences between the properties obtained by Silva et al. (1995) and those predicted in this study may have resulted from the use of different types of boundary conditions, as mentioned in Section 2.2.

3.4. Effects of cell wall thickness non-uniformity

For two-dimensional foams, the influence of cell wall thickness variations on the elastic properties is still unclear. The regular honeycombs with $a = 0$, the irregular honeycombs with $a = 0.5$ and the completely irregular honeycombs with $a = 1.0$, all having non-uniform cell wall thickness, are therefore analyzed here. Four values of the thickness non-uniformity amplitude, i.e., $b = 0.2$, 0.5, 0.8 and 1.0, are used for each of the three values of a. When $b = 1.0$, cell wall thickness variations are completely random. For each pair of a and b, 20 honeycomb samples are modeled using independent lists of random variables θ_i, φ_i ($i \in \{1, \ldots, M\}$) and ψ_j ($j \in \{1, \ldots, N\}$). The relative density R remains to be 0.01 for the samples analyzed here, and more samples with different values of R will be discussed in Section 3.5.

The predicted effective elastic properties are shown in Figs. 11–13. Figs. 11 and 12 reveal that the Young's moduli and shear modulus significantly decrease in a monotonic fashion as b increases for all three

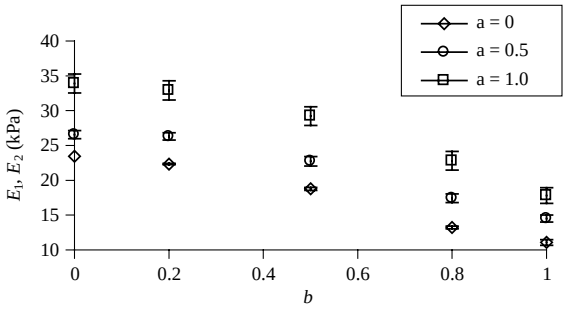

Fig. 11. Effects of cell wall thickness variations on the Young's moduli (with $R = 0.01$).

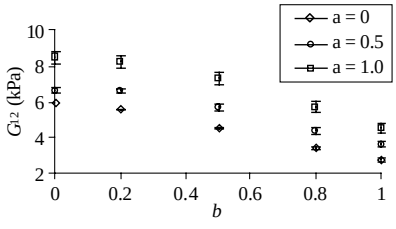

Fig. 12. Effects of cell wall thickness variations on the shear modulus (with $R = 0.01$).

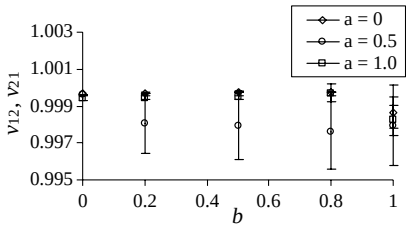

Fig. 13. Effects of cell wall thickness variations on the Poisson's ratios (with $R = 0.01$).

values of a considered. For the regular honeycombs ($a = 0$), the Young's moduli and shear modulus are reduced by about 53% as b changes from 0 to 1.0, while the relative reduction is approximately 47% for the fully irregular honeycombs ($a = 1.0$) and 45% for the irregular honeycombs with $a = 0.5$. The Poisson's ratios, however, are negligibly influenced in each case by the values of a, as shown in Fig. 13.

An inspection of Figs. 11 and 12 also indicates that for each value of b the elastic moduli are the highest for the completely irregular honeycomb with $a = 1.0$, the second highest for the irregular honeycomb with $a = 0.5$, and the lowest for the regular honeycomb with $a = 0$. This is because irregular cell shapes result in polyhedrons with higher stiffness than hexagons, as noted earlier. Furthermore, it can be seen that the differences between the mean values of the elastic moduli for each two of the three types of honeycombs with $a = 1.0$, $a = 0.5$ and $a = 0$ are insignificantly affected by varying b. This implies that the effect of the interaction between the cell shape and cell wall thickness variations on the elastic properties of each honeycomb is weak. When these two variations are very small (i.e., $a \ll 1, b \ll 1$), the weak interaction observed here can be analytically shown to be true (Grenestedt, 2003) for any such imperfect honeycomb with a given value of R by using a power series based technique initially proposed in Grenestedt and Tanaka (1999) for 3-D closed-cell foams with irregular cell shapes.

A further examination of Figs. 11 and 12 shows that the elastic moduli are affected more by the cell wall thickness non-uniformity than by the cell shape irregularity. This follows from the fact that the elastic properties for the cases with $a = 1.0$, $b = 1.0$ and $a = 0.5$, $b = 0.5$ are smaller than the corresponding ones for the case with $a = 0$, $b = 0$ (i.e., honeycombs without imperfections), although the elastic moduli are found to increase as a increases (for fixed b) and to decrease with the increase of b (for fixed values of a), as discussed earlier. Moreover, for the special cases without the interaction (i.e., with a or b being zero but the other one varying), it is found that the maximum gain of moduli is 45% as a varies from 0 to 1.0 with the cell wall thickness being uniform (i.e., $b = 0$), as mentioned in Section 3.3, while the maximum loss of moduli is 53% as b changes from 0 to 1.0 for a regular honeycomb (with $a = 0$). These observations based on the simulation results for the honeycombs with $R = 0.01$ are supported by the numerical data obtained for imperfect honeycombs with different values of R, which will be discussed next.

3.5. Effects of the relative density

Figs. 14–16 show the results of the effective Young's moduli, shear modulus and Poisson's ratios as a function of the relative density for four types of honeycombs: the regular honeycombs with a uniform cell wall thickness ($a = 0, b = 0$), the completely irregular honeycombs with a uniform cell wall thickness ($a = 1.0, b = 0$), the regular honeycombs with completely non-uniform cell wall thickness ($a = 0, b = 1.0$), and the completely irregular honeycombs with completely non-uniform cell wall thickness ($a = 1.0$, $b = 1.0$).

For the honeycombs with a uniform cell wall thickness (i.e., $b = 0$), the relative density (R) depends on the cell wall thickness, as dictated by Eq. (2). The relative density of the irregular honeycombs (with $b \neq 0$)

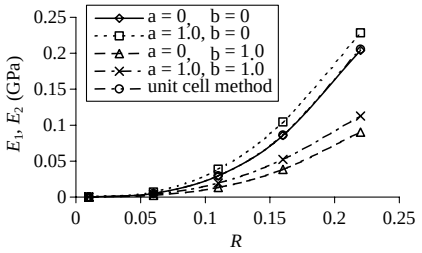

Fig. 14. Effects of the relative density on the Young's moduli.

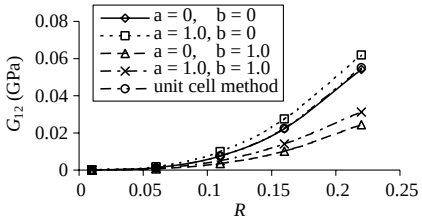

Fig. 15. Effects of the relative density on the shear modulus.

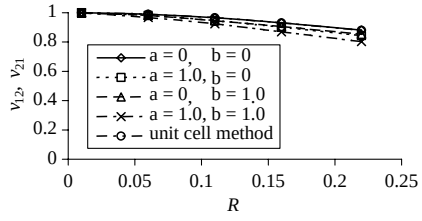

Fig. 16. Effects of the relative density on the Poisson's ratios.

depends not only on the cell wall thickness (and its variations) but also on cell shapes, as governed by Eqs. (2)–(4). Five relative densities, i.e., $R = 0.01$, 0.06, 0.11, 0.16 and 0.22, are used for each type of the honeycombs listed above. For the perfect honeycomb (i.e., $a = 0, b = 0$) only one model is needed for each density. For the remaining three types of honeycombs with shape and/or thickness imperfections, 20 models are built for each density except for the case with $R = 0.01$, which has been dealt with in the simulations discussed earlier. The statistical distributions of θ_i, φ_i ($i \in \{1,\ldots,M\}$) and ψ_j ($j \in \{1,\ldots,N\}$) remain the same for the models with $R = 0.06$, 0.11, 0.16 and 0.22 as those for the models with $R = 0.01$.

It appears that the effective Young's moduli and shear modulus of each of the four types of honeycombs vary as a power-law function of the relative density, as shown in Figs. 14 and 15. These variations can be captured by the power-law regression equations listed in Table 4, where the regression formula for the unit cell-based micromechanics model of Silva et al. (1995) (see Eqs. (12)–(14)) is also included for comparison. An inspection of Table 4 shows that the two non-dimensional Young's moduli of all the four types of honeycombs have very similar forms of regression equations, which again confirms the isotropy of honeycombs as measured by the Young's moduli. Hence, it suffices to discuss the regression equations for E_1/E_s alone in the remaining part of this section.

Clearly, the unit-cell based model of Silva et al. (1995), which incorporates bending as well as stretching and shearing effects, is accompanied by a power-law exponent of 2.94909, which is less than 3.0, the value

Table 4
Power-law regression equations for the elastic moduli

	E_1/E_s	E_2/E_s	G_{12}/E_s
$a = 0.0$, $b = 0.0$	$1.21028R^{2.94683}$	$1.21028R^{2.94683}$	$0.32331R^{2.96321}$
$a = 1.0$, $b = 0.0$	$1.29147R^{2.87270}$	$1.29452R^{2.87327}$	$0.35454R^{2.89555}$
$a = 0.0$, $b = 1.0$	$0.52653R^{2.92731}$	$0.52516R^{2.92697}$	$0.14342R^{2.94822}$
$a = 1.0$, $b = 1.0$	$0.62298R^{2.85256}$	$0.62483R^{2.85342}$	$0.17427R^{2.87643}$
Unit cell method (Silva et al., 1995)	$1.22142R^{2.94909}$	$1.22142R^{2.94909}$	$0.32893R^{2.96747}$

that was obtained by considering bending as the only deformation mechanism (Gibson and Ashby, 1997). For the perfect honeycomb (with $a = 0, b = 0$) simulated here, the exponent of its regression equation, 2.94683, is very close to 3.0. This reduction of 1.8% (from 3.0) reflects the effects of stretching and shearing deformations, which agrees with what is revealed by comparing the model of Silva et al. (1995) with that of Gibson and Ashby (1997), as noted above. The power-law exponent reaches its maximum value (i.e., 2.94683) for the perfect honeycomb and its minimum value (i.e., 2.85256) for the completely random honeycombs (with $a = 1.0, b = 1.0$). This implies that the presence of shape and/or thickness imperfections fosters the effects of stretching and shearing deformations. By comparing the power-law exponents for honeycombs with $a = 1.0, b = 0$ and those with $a = 0, b = 1.0$, one can find that shape irregularity weakens bending deformations more than thickness non-uniformity does. Since the minimum power-law exponent for the completely random honeycombs, 2.85256, is only 4.9% less than 3.0, it can be concluded that bending still dominates deformations of honeycombs having shape and/or thickness imperfections. On the other hand, the coefficient of each regression equation measures the Young's modulus of the honeycombs relative to E_s for a given value of R. The fact that the coefficient for the perfect honeycomb (with $a = 0$ and $b = 0$), i.e., 1.21028, is less than the one for the honeycombs with $a = 1.0$ and $b = 0$, i.e., 1.29147, and greater than the one for the honeycombs with $a = 0$ and $b = 1.0$, i.e., 0.526533, indicates that the Young's modulus (E_1) is enhanced by the shape irregularity but undermined by the thickness non-uniformity. A smaller coefficient for the completely random honeycombs with $a = 1.0$ and $b = 1.0$, i.e., 0.62298, than that for the perfect honeycomb (i.e., 1.21028) implies that the stiffness-strengthening effect caused by the shape irregularity is less pronounced than the stiffness-weakening effect due to the thickness non-uniformity. These observations agree with those made earlier based on Figs. 7 and 11 about the Young's modulus varying with a and/or b for fixed R. It can be further shown that how the relative density affects the shear modulus is similar to that for the Young's moduli discussed here.

Fig. 16 illustrates the relations of the Poisson's ratios varying with the relative density R. For all of the four types of honeycombs, both v_{12} and v_{21} decrease moderately with the increase of R in a monotonic manner. It is seen that the influence of a and b on v_{12} and v_{21} is insignificantly small at various values of R considered, which, again, is in agreement with the earlier observations based in Figs. 9 and 13 (for fixed R).

In order to further explore the effects of the relative density (R) on the behavior of foams having the two co-existing imperfections, the differences between the elastic properties of the imperfect foams and those of the perfect foams (with $a = 0, b = 0$) are calculated. The differences are given by

$$e_Q = Q^r - Q^p \tag{16}$$

where e_Q is the difference, Q denotes the elastic modulus (E_1, E_2 or G_{12}), and the superscripts r and p stand for, respectively, the random and perfect honeycombs. The numerical results for e_Q as a function of R are illustrated in Figs. 17 and 18.

It is observed from Figs. 17 and 18 that when R increases the differences in the three elastic moduli induced by the presence of irregular cell shapes increase, while those by the non-uniform cell wall thickness decrease, both in a monotonic manner. A further examination of Figs. 17 and 18 reveals that when R is small the increase in the moduli due to the cell shape irregularity (i.e., $a \neq 0$) is slightly smaller than the

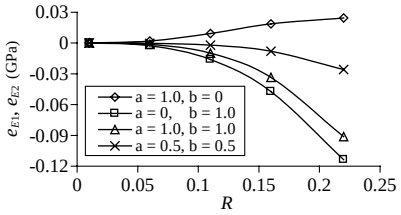

Fig. 17. Differences in the Young's moduli varying with the relative density.

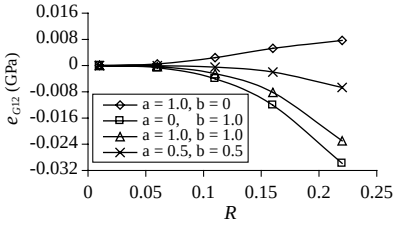

Fig. 18. Differences in the shear modulus varying with the relative density.

decrease in the moduli due to the cell wall thickness non-uniformity (i.e., $b \neq 0$). When R becomes large, however, the effects of the cell wall thickness non-uniformity on the elastic moduli are more significant than those by the cell shape irregularity. As a result, the elastic moduli of the honeycombs with the two co-existing imperfections are lower than those of the perfect honeycombs and the differences between them increase with R, as illustrated in Figs. 17 and 18. These observations support and enhance those based in Figs. 11 and 12 for honeycombs with $R = 0.01$.

4. Summary

The effects of co-existing cell shape and cell wall thickness imperfections on the elastic properties of 2-D cellular solids (honeycombs) are studied using the Voronoi tessellation technique and the finite element method. Voronoi diagrams with different degrees of cell shape irregularity (amplitude a) are produced by perturbing a regular packing of seeds. Perturbations are then introduced to the uniform thickness of the cell walls to generate a uniform distribution of wall thickness with different degrees of non-uniformity (amplitude b). Twenty finite element (FE) models are constructed, based on the Voronoi diagrams for 20 honeycomb samples having the same pair of a and b, to obtain the mean values and standard deviations of the effective elastic properties. Each sample contains 360 complete cells.

Based on the simulation results and analyses presented, the following conclusions can be drawn:

(1) The elastic response of honeycombs with co-existing cell shape and cell wall thickness imperfections appears to be isotropic regardless of changes in the cell shape irregularity (a), the cell wall thickness non-uniformity (b) and the relative density (R). The differences between the elastic properties associated with different FE models (with the same pair of a and b) increase as cells become more irregular and the relative density larger.
(2) For irregular honeycombs with cell walls of uniform thickness, as the cell shapes become more irregular, on average, the elastic moduli increase considerably, while the Poisson's ratios are insignificantly affected.

(3) For regular honeycombs, the increase in the cell wall thickness non-uniformity substantially reduces the elastic moduli but has little influence on the effective Poisson's ratios.
(4) When irregular cell shapes and non-uniform cell wall thickness co-exist in a honeycomb, the effect of the interaction between the two types of imperfections on the elastic properties is found to be weak. The stiffness gain resulting from the appearance of irregular cells is less than the stiffness loss due to the perturbation to the uniform cell wall thickness when the value of a (measuring the cell shape irregularity) and the value of b (measuring the cell wall thickness non-uniformity) are the same. Consequently, the elastic moduli of the honeycombs with the two co-existing imperfections are lower than those of the perfect honeycombs, and the differences increase when the value of R becomes large.
(5) With variations in cell shapes and cell wall thickness, the elastic moduli of imperfect honeycombs vary as a power-law function of the relative density. Bending is still the dominant deformation mechanism. The contributions of stretching and shearing, even after being strengthened by cell shape and cell wall thickness imperfections, only reduce the power-law exponent by a few percent. The Poisson's ratios decrease insignificantly as the relative density increases.

Acknowledgments

The work reported here is partially funded by a grant from the AFOSR (Grant # F49620-03-1-0004) and by a contract from L&L Products. These supports are gratefully acknowledged. The public access to the Qhull program initially made available by the Geometry Center at the University of Minnesota—Twin Cities is also deeply appreciated. In addition, the authors wish to thank Professor C. R. Steele and two anonymous reviewers for their critical and helpful comments on an earlier version of this paper, which have led to significant improvements of the paper.

References

Chen, C., Lu, T.J., Fleck, N.A., 1999. Effect of imperfections on the yielding of two-dimensional foams. J. Mech. Phys. Solids 47, 2235–2272.

Fazekas, A., Dendievel, R., Salvo, L., Brechet, Y., 2002. Effect of microstructural topology upon the stiffness and strength of 2D cellular structures. Int. J. Mech. Sci. 44, 2047–2066.

Gibson, L.J., Ashby, M.F., 1997. Cellular Solids: Structures and Properties, second ed. Cambridge University Press, Cambridge.

Glaessgen, E.H., Phillips, D.R., Iesulauro, E., Saether, E., Piascik, R.S., 2003. A multiscale approach to modeling fracture in metallic materials containing nonmetallic inclusions. AIAA 2003-1616. American Institute of Aeronautics and Astronautics, Reston, VA.

Grenestedt, J.L., 2003. Personal communications.

Grenestedt, J.L., Bassinet, F., 2000. Influence of cell wall thickness variations on elastic stiffness of closed-cell cellular solids. Int. J. Mech. Sci. 42, 1327–1338.

Grenestedt, J.L., Tanaka, K., 1999. Influence of cell shape variations on elastic stiffness of closed cell cellular solids. Scr. Mater. 40, 71–77.

Hibbitt, Karlson, Sorenson, Inc., 2002. ABAQUS Theory and User's Manuals, Version 6.3. Hibbitt, Karlson and Sorenson, Inc., Pawtucket, RI.

Kanit, T., Forest, S., Galliet, I., Mounoury, V., Jeulin, D., 2003. Determination of the size of the representative volume element for random composites: statistical and numerical approach. Int. J. Solids Struct. 40, 3647–3679.

Laroussi, M., Sab, K., Alaoui, A., 2002. Foam mechanics: nonlinear response of an elastic 3D-periodic microstructure. Int. J. Solids Struct. 39, 3599–3623.

Li, K., Gao, X.-L., Roy, A.K., 2003a. Micromechanics model for three-dimensional open-cell foams using a tetrakaidecahedral unit cell and Castigliano's second theorem. Compos. Sci. Tech. 63, 1769–1781.

Li, K., Gao, X.-L., Roy, A.K., 2003b. Micromechanical analysis of three-dimensional open-cell foams using the matrix method for space frame structures. Proc. 14th Int. Conf. on Composite Materials (ICCM-14), July 14–18, 2003, San Diego, CA.

Nygards, M., Gudmundson, P., 2002. Micromechanical modeling of ferritic/pearlitic steels. Mater. Sci. Eng. A 24, 435–443.
Silva, M.J., Gibson, L.J., 1997. The effects of non-periodic microstructure and defects on the compressive strength of two-dimensional cellular solids. Int. J. Mech. Sci. 39, 549–563.
Silva, M.J., Hayes, W.C., Gibson, L.J., 1995. The effects of non-periodic microstructure on the elastic properties of two-dimensional cellular solids. Int. J. Mech. Sci. 37, 1161–1177.
Simone, A.E., Gibson, L.J., 1998a. Effects of solid distribution on the stiffness and strength of metallic foams. Acta Mater. 46, 2139–2150.
Simone, A.E., Gibson, L.J., 1998b. The effects of cell face curvature and corrugations on the stiffness and strength of metallic foams. Acta Mater. 46, 3929–3935.
Van der Burg, M.W.D., Shulmeister, V., Van der Geissen, E., Marissen, R., 1997. On the linear elastic properties of regular and random open-cell foam models. J. Cell. Plastics 33, 31–54.